

Omni IIE Bench: Benchmarking the Practical Capabilities of Image Editing Models

Yujia Yang^{1*}, Yuanxiang Wang¹, Zhenyu Guan¹, Tiankun Yang¹, Chenxi Bao¹
 Haopeng Jin², Jinwen Luo², Xinyu Zuo², Lisheng Duan²
 Haijin Liang², Jin Ma², Xinming Wang², Ruiwen Tao², Hongzhu Yi^{1*†}
¹University of Chinese Academy of Sciences, ²Tencent
<https://github.com/Young-2000/OmniIIEBench>

Abstract

While Instruction-based Image Editing (IIE) has achieved significant progress, existing benchmarks pursue task breadth via mixed evaluations. This paradigm obscures a critical failure mode crucial in professional applications: the inconsistent performance of models across tasks of varying semantic scales. To address this gap, we introduce **Omni IIE Bench**, a high-quality, human-annotated benchmark specifically designed to diagnose the editing consistency of IIE models in practical application scenarios. **Omni IIE Bench** features an innovative dual-track diagnostic design: (1) **Single-turn Consistency**, comprising shared-context task pairs of attribute modification and entity replacement; and (2) **Multi-turn Coordination**, involving continuous dialogue tasks that traverse semantic scales. The benchmark is constructed via an **exceptionally rigorous** multi-stage human filtering process, incorporating a quality standard enforced by computer vision graduate students and an industry relevance review conducted by professional designers. We perform a comprehensive evaluation of 8 mainstream IIE models using **Omni IIE Bench**. Our analysis quantifies, for the first time, a prevalent performance gap: nearly all models exhibit a significant performance degradation when transitioning from low-semantic-scale to high-semantic-scale tasks. **Omni IIE Bench** provides critical diagnostic tools and insights for the development of next-generation, more reliable, and stable IIE models.

1. Introduction

In recent years, the capabilities of multimodal image editing models [2, 3, 7, 10, 16, 31, 32, 45, 47] have been continuously improving, driving the development

of Instruction-based Image Editing (IIE) tasks. IIE models enable users to iteratively manipulate image content through natural language. This simple and intuitive editing paradigm greatly enhances the flexibility and interactivity of visual creation, rapidly becoming a core tool in the design domain.

Early IIE benchmarks primarily focused on single-turn dialogues [1, 18, 24, 26, 27, 38, 40, 41], evaluating whether models could produce high-quality edits based on a single instruction. During this stage, editing instructions were mainly categorized into attribute modifications and entity modifications. However, single-turn settings overlook the importance of multi-turn interactions in real design workflows.

Recent studies have begun to explore multi-turn editing [11, 33, 36, 37, 42, 43, 48], but they are typically limited to 2–3 rounds of dialogue. In contrast, in practical design processes, designers tend to perform edits frequently and progressively, refining images through multiple iterations. Therefore, 2–3 rounds of interaction are insufficient to accurately assess a model’s true practical capability.

More importantly, existing IIE benchmarks have not been validated by experienced designers, leading to a noticeable gap between idealized benchmark performance and practical applicability.

To systematically evaluate the large-scale applicability of different IIE models in practical scenarios, it is thus essential to establish a diagnostic benchmark grounded in real design practice. To address these challenges, this paper proposes **Omni IIE Bench** — a rigorously human-evaluated benchmark designed to diagnose the practical performance of IIE models. The main contributions of this work are as follows:

1. High-quality evaluation dataset: We propose a high-quality evaluation dataset consisting of both single-turn and multi-turn dialogue data. The single-turn dataset contains 1,725 image editing dialogues, while

*Equal contribution.

†Corresponding Author.

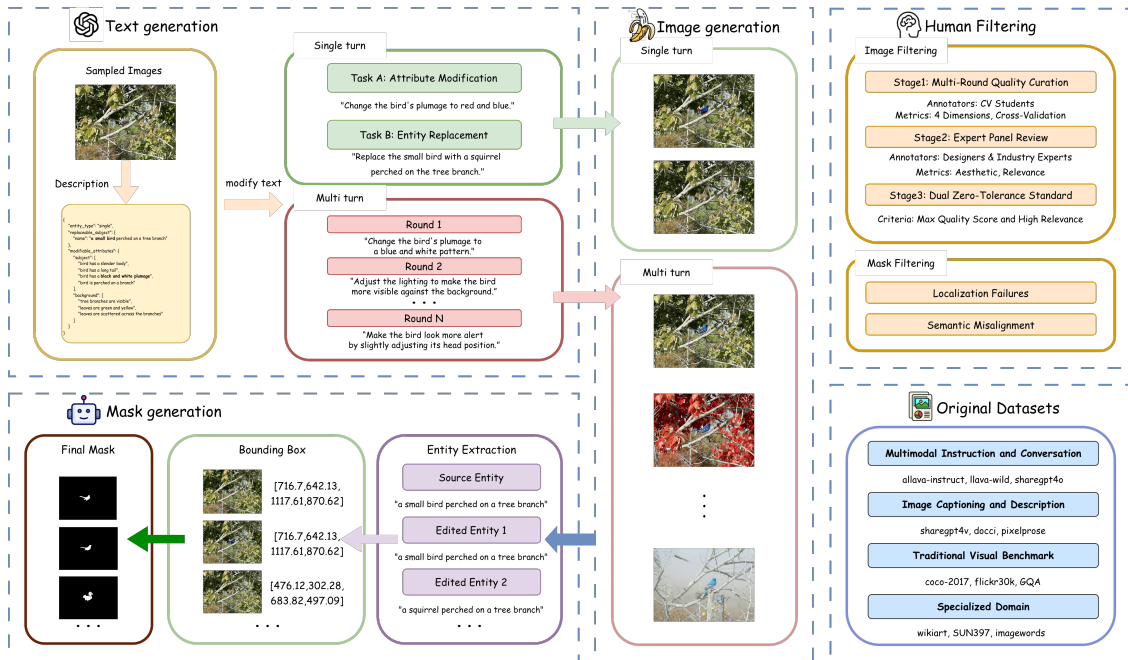


Figure 1. Omni IIE Bench collects seed images from 12 datasets and uses *GPT-4o* to generate image descriptions. The descriptions are then randomly modified by *GPT-4o*. For single-turn dialogue generation, semantic scales are done at low and high levels; for multi-turn dialogue generation, modifications are randomly interleaved between the two levels. After that, the original descriptions, modified descriptions, and original images are input into *Nano Banana* for image generation, and the results are processed with *GroundingDINO* and *SAM* to obtain masks. Finally, all generated images and masks undergo strict manual review.

the multi-turn dataset includes 260 multi-round dialogues, with up to 16 turns per dialogue. The dataset was constructed with extensive human involvement and a rigorous data filtering process to ensure quality and reliability.

2. Decoupled and robust evaluation methodology:

We introduce a decoupled diagnostic evaluation framework that assesses model performance along three key dimensions: global image quality, decoupled regional fidelity, and instruction compliance. This framework provides a more interpretable and fine-grained evaluation of editing performance than traditional single-score methods.

3. Systematic diagnostic analysis of mainstream IIE models:

Using our proposed benchmark, we conduct a comprehensive evaluation of several mainstream IIE models, revealing their actual performance in practical scenarios. Furthermore, we perform human validation of the evaluation results, which show a high degree of consistency with automated assessments, demonstrating the effectiveness and reliability of Omni IIE Bench.

2. Related Work

Single-turn Evaluation Benchmarks: Existing single-turn benchmarks tend to pursue task coverage by evaluating a mixture of tasks, thereby testing overall

model capability [1, 18, 24, 27, 28, 35, 46]. However, this mixed evaluation paradigm obscures the specific performance differences of models across different semantic-scale tasks. I2EBench [18], for example, attempts to explicitly separate *high-level* and *low-level* edits through a hierarchical design, which underscores the importance of the semantic scale concept. Yet, it also adopts an isolated checklist-style evaluation, assessing and reporting performance separately for different task levels, without diagnosing model stability when handling cross-scale task switching in the same image context.

Multi-turn Evaluation Benchmarks: Other multi-turn benchmarks focus on evaluating *temporal consistency* during the editing process [11, 29, 37, 43, 48–50]. Although CompBench [11] supports multi-turn editing and distinguishes four dimensions in its instruction decoupling strategy, it still reports each task score as an isolated metric, failing to quantify model consistency between low and high semantic scale tasks. ImgEditBench [37] emphasizes assessing content memory, content understanding, and version rollback abilities. Similarly, MUCIE [48] concentrates on instruction retention and reasoning memory to mitigate error accumulation. While these studies are crucial for interactive editing,

they do not consider model stability and coordination when the semantic scale of editing tasks dynamically changes.

3. Omni IIE Bench Dataset

Constructing a practical benchmark for diagnosing **Instruction-based Image Editing (IIE)** models is a challenging engineering task. As shown in Figure 1 and Table 1, we propose **Omni IIE Bench**, a benchmark for evaluating practical image editing, rigorously reviewed through manual assessment.

Omni IIE Bench features two core attributes:

Diagnostic Power. It provides complementary single-turn and multi-turn diagnostic tracks to assess models’ semantic understanding, editing consistency, and stability across iterative modifications.

Strict Review. Seed images are drawn from 12 public datasets. All generated editing instructions and edited images are manually reviewed by professional designers and computer vision researchers to ensure that the data aligns with practical application scenarios.

3.1. Data Acquisition and Sourcing

To ensure the benchmark’s diversity and practical scene coverage, our initial image pool is sampled from 12 public datasets, categorized by content and style into four types:

- **Multimodal Instruction and Conversation:** allava-instruct [4], llava-wild [14], sharegpt4o [5]
- **Image Captioning and Description:** sharegpt4v [6], docci [19], pixelprose [25]
- **Traditional Visual Benchmark:** coco2017val [13], flickr30k [39], GQA [9]
- **Specialized Domain:** wikiart [23], SUN397 [34], imageinwords [8]

All sampling processes use a fixed random seed $seed = 42$ to ensure reproducibility. We constructed independent seed pools for the two diagnostic tracks. For the **single-turn consistency seed pool**, we randomly sampled 200 images from each of the 12 datasets, forming a 2,400-image main seed pool. For the **multi-turn coordination seed pool**, we randomly sampled 58 images from each dataset, forming a 696-image multi-turn dialogue seed pool, used to construct continuous, multi-scale editing dialogues.

3.2. Data Generation and Annotation Pipeline

To ensure that Omni IIE Bench is both scientifically rigorous and aligned with practical application scenarios, we established detailed annotation type definitions and constructed a three-stage data generation and filtering pipeline.

3.2.1. Annotation Types

All samples are organized as quadruplets $(I_{source}, T_{mod}, I_{gt}, M_{gt})$, where I_{source} is the source image, T_{mod} is the editing instruction, I_{gt} is the target image, and M_{gt} is the ground-truth mask.

Multi-Turn Diagnosis. Contains 696 sets of cross-scale multi-turn dialogues. Each set simulates a user’s continuous interaction with the model, with instructions dynamically interspersing **attribute modification** and **entity replacement**, to evaluate the model’s contextual understanding, instruction coordination, and error accumulation capabilities in continuous editing.

3.2.2. Generation and Annotation Process

Stage 1: Automated Candidate Data Generation

This stage utilizes advanced vision-language and generative models to automatically generate candidate data.

- (1) **Image Captioning:** We use the gpt-4o[20] model to generate fine-grained scene descriptions for the 2,400 main seed pool images and the 696 multi-turn dialogue seed pool images, covering target objects, attributes, actions, and environmental relationships.
- (2) **Instruction Generation:** The gpt-4o model then generates editing instruction sets based on these scene descriptions. For single-turn consistency diagnosis, it generates dual-task instruction pairs with opposing semantics. For multi-turn coordination, it generates multi-turn instruction sequences that alternate across semantic scales.
- (3) **GT Image Generation:** We employ Nano Banana [17] to ensure the high fidelity of the ground-truth image generation.

Stage 2: Automated Mask Generation

The core task of this stage is to automatically generate high-quality ground-truth masks for all generated candidate samples, ensuring spatial alignment with the instruction’s intent.

- (1) **Instruction Parsing:** Directly inputting the full natural language instruction T_{mod} into GroundingDINO [15] is infeasible, as it requires clear entity nouns. Therefore, we designed an instruction parsing step. We utilize gpt-4o as the instruction parser. The parser’s task is to analyze the intent of T_{mod} and extract only the core entity noun being edited. For attribute modification tasks, the parser likewise extracts its carrier; for entity replacement tasks, it extracts the original entity being replaced.
- (2) **Mask Extraction:** After instruction parsing, the extracted entity nouns are passed as text prompts to the Grounded-SAM framework [22] for fully automated mask extraction. The process first activates the GroundingDINO module to receive the entity nouns, and its output candidate bounding boxes are passed as spatial prompts to the SAM module [12]. SAM finally performs high-precision instance segmentation based on

Table 1. Comparison of IIE Benchmarks on Key Diagnostic Dimensions.

Benchmark	Human Verified	Provides Mask	Practical Scenarios	Semantic Scale	Dialogue Length
I2EBench [18]	✓	✓	✗	✓	1
EditBench [27]	✓	✓	✗	✓	1
EditVal [1]	✓	✗	✗	✗	1
EmuEdit [24]	✓	✗	✗	✗	1
AnyEdit [40]	✗	✓	✗	✗	1
CompBench [11]	✓	✓	✗	✗	2
MagicBrush [43]	✓	✗	✗	✗	3
ImgEdit-Bench [37]	✓	✗	✗	✗	3
MuCIE [48]	✗	✗	✗	✗	5
Omni IIE Bench (Ours)	✓	✓	✓	✓	16

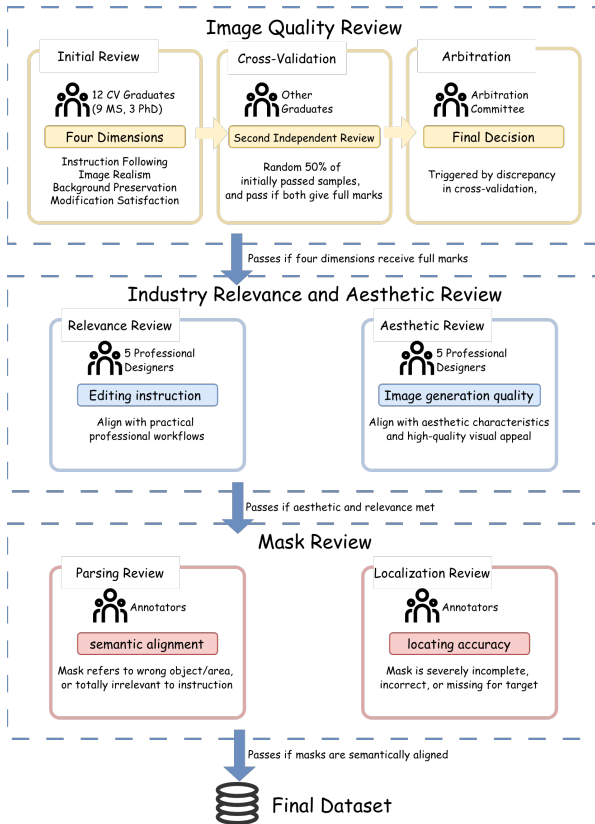


Figure 2. Overview of manual curation and filtering

these spatial prompts, generating the binarized ground-truth mask M_{gt} .

Stage 3: Manual Curation and Filtering This stage is the most critical juncture for ensuring the final quality of Omni IIE Bench benchmark. To fully leverage our team’s professional capabilities, we designed a hierarchical, multi-pass manual quality assessment process. An overview of the manual curation and filtering process can be found in Figure 2.

Annotation Team and Calibration. The annotation team includes 12 CV graduate students and 5 AI image editing designers. Before formal annotation, all

members undergo a calibration phase to align on detailed guidelines and key metrics such as artifacts, semantic drift, and background pollution, ensuring consistent evaluation standards. Each candidate sample is manually scored from 1 to 3 on four dimensions:

Image Quality Review. Each candidate sample is first manually scored from 1 to 3 on four dimensions:

- **Instruction Following:** Adherence to the editing instruction.
- **Image Realism:** Naturalness and absence of obvious artifacts.
- **Background Preservation:** Integrity of unedited regions.
- **Modification Satisfaction:** Overall acceptability of the editing result.

This review follows a rigorous workflow: (1) **Annotator Initial Review:** 9 master’s and 3 PhD annotators independently score each sample across the four dimensions. (2) **Cross-Validation and Arbitration:** To ensure quality, 50% of initially passed samples are randomly selected for a second independent review by another annotator. If both annotators give full marks, the sample passes; if there is a discrepancy, it is submitted to an Arbitration Committee of 5 designers, who make the final decision through discussion and voting.

Industry Relevance and Aesthetic Review. All samples that passed the initial quality check are then entered into an independent industry relevance and aesthetic review stage. This stage is conducted by a Review Team of 5 professional designers proficient in AI image editing software. The Review Task involves the expert team re-evaluating the image generation quality and the editing instruction T_{mod} itself, assessing whether they align with practical professional workflows and aesthetic characteristics in areas such as advertising design, e-commerce, or film concept art. The Filtering Criteria are based on the expert team’s subjective assessment of the instruction’s industry relevance and aesthetic characteristics, and samples deemed not to meet practical work requirements are removed.

Mask Review. After the automated mask generation,

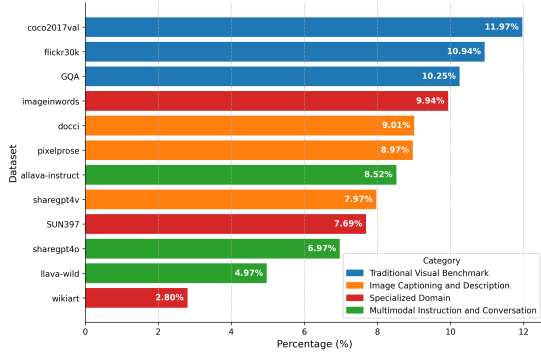


Figure 3. Source Distribution of Datasets in Omni IIE Bench

the masks undergo a rapid manual review. This step is not for pixel-level correction; annotators only make a Pass or Fail judgment on the semantic alignment of the mask with the instruction. The sole purpose of this is to filter out samples with severe misalignment caused by parsing errors or GroundingDINO localization failures.

Final Filtering Criteria. We employ an extremely strict dual zero-tolerance filtering standard. A sample must meet both of the following conditions to be accepted into the final Omni IIE Bench benchmark: (1) **Quality Standard:** Judged to have received full marks on all four dimensions in the Image Quality Review. (2) **Relevance Standard:** Judged as Relevant by the professional designer team in the Industry Relevance and Aesthetic Review. This rigorous dual standard, combined with the mask review, ensures every sample is high-quality, relevant, and spatially valid. Ultimately, we were left with 2856 images.

3.3. Data Statistics

3.3.1. Curation Pipeline and Source Distribution

Curation Pipeline. We employed a rigorous, zero-tolerance filtering standard across both diagnostic tracks. For the single-turn track, from 4,800 initial candidate samples, only 50.86% passed the multi-dimensional quality review. Of those, an additional 29.33% were subsequently discarded by industry experts for lacking practical relevance, resulting in a final acceptance rate of just 35.94%, yielding 1,725 samples. For the multi-turn track, from 696 initial dialogue groups containing 5,421 images, a similar filtering process yielded 260 final groups, which represents a 37.36% acceptance rate for groups, and 1,131 final images, representing a 20.86% acceptance rate for images. This multi-stage process, with a combined final acceptance of 2,856 images from 10,221 initial candidates, ensures the reliability and practical value of the final Omni IIE Bench.

Source Distribution. As shown in Figure 3, our benchmark is sourced from 12 distinct datasets. The distribution is well-balanced, with the largest single source accounting for only 11.97% of the data. This balanced mix ensures our evaluation is not biased towards any single data type and robustly covers diverse scenarios.

3.3.2. Diagnostic Attribute Analysis

Mask Attributes. Mask area statistics validate our division of semantic scales. We find that attribute modification tasks’ mask areas tend to be concentrated in a small range, while entity replacement tasks’ mask areas are more broadly distributed.

Multi-Turn Coordination Attributes. The multi-turn track contains 260 dialogue groups with an average depth of 4.35 turns. Within the 1,131 total editing turns, we recorded 322 attribute-to-entity and 178 entity-to-attribute scale switches, ensuring thorough testing of dynamic, cross-scale coordination.

4. Evaluation Methodology

To fairly and comprehensively evaluate IIE models, we propose a decoupled diagnostic evaluation framework. Our methodology decouples the evaluation into three core dimensions: (1) **Global Image Quality**, (2) **Decoupled Regional Fidelity**, and (3) **Instruction Compliance**. This section will detail our evaluation pipeline and all metrics used.

4.1. Evaluation Pipeline and Preprocessing

Our evaluation pipeline loads samples from a JSON manifest, which provides paths to the source image I_{source} , the ground-truth target image I_{gt} , and the ground-truth mask M_{gt} . To ensure all comparisons are conducted on a uniform scale, we define a strict preprocessing step. All images are resampled to a standard resolution of (768, 768) using lanczos interpolation. All masks are similarly resampled to (768, 768), but using nearest interpolation to preserve the sharpness of their binary boundaries. We define the foreground mask $M_{fg} = M_{gt}$ and the background mask $M_{bg} = 1 - M_{gt}$. All decoupled metrics are computed on these specific regions.

4.2. Global Image Quality Metrics

This dimension assesses the overall quality of I_{gen} compared to I_{gt} . We employ four standard metrics: **PSNR** and **SSIM** [30] evaluate pixel-level fidelity and structural similarity. **LPIPS** [44] measures perceptual similarity. It is computed as a weighted distance between deep features F from network layers l , where H_l and W_l are the feature map dimensions, $\sum_{h,w}$ iterates over all spatial positions, and \odot denotes element-wise multi-

Table 2. Performance comparison of IIE models on a single turn. Text colors indicate top performances: 1st, 2nd, 3rd. Arrows (\uparrow / \downarrow) indicate whether higher or lower values are better. The Overall score is calculated by the formula $\frac{1}{4} \left[\frac{3 - (\sum \text{LPIPS})}{3} + \frac{\sum \text{CLIP}}{3} + \text{QA} + \text{SSIM} \right]$, where $\sum \text{LPIPS}$ and $\sum \text{CLIP}$ are the sums of their respective FG, BG, and ALL columns.

Model	LPIPS (\downarrow)			CLIP (\uparrow)			QA (\uparrow)	Image Quality (\uparrow)		Overall
	FG	BG	ALL	FG	BG	ALL		PSNR	SSIM	
Qwen-image-edit[32]	0.245	0.327	0.450	0.887	0.891	0.889	0.744	14.401	0.455	0.687
InstructPix2Pix[3]	0.284	0.441	0.569	0.774	0.775	0.841	0.316	12.423	0.438	0.530
ICEdit[47]	0.252	0.295	0.425	0.867	0.875	0.868	0.453	15.541	0.507	0.626
MGIE[7]	0.261	0.294	0.426	0.858	0.864	0.859	0.070	14.733	0.480	0.520
HIVE[45]	0.287	0.406	0.526	0.849	0.796	0.794	0.259	13.423	0.414	0.527
FLUX[2]	0.283	0.428	0.552	0.863	0.871	0.868	0.636	12.553	0.375	0.614
HQEdit[10]	0.327	0.557	0.689	0.794	0.691	0.694	0.322	9.259	0.304	0.457
Step1X[16]	0.230	0.259	0.379	0.887	0.903	0.899	0.580	15.845	0.533	0.680

Table 3. Performance comparison of IIE models on multi turns. Text colors indicate top performances: 1st, 2nd, 3rd. Arrows (\uparrow / \downarrow) indicate whether higher or lower values are better.

Model	LPIPS (\downarrow)			CLIP (\uparrow)			QA (\uparrow)	Image Quality (\uparrow)		Overall
	FG	BG	ALL	FG	BG	ALL		PSNR	SSIM	
Qwen-image-edit	0.254	0.390	0.510	0.888	0.879	0.877	0.818	13.521	0.391	0.676
InstructPix2Pix	0.296	0.552	0.669	0.842	0.701	0.703	0.560	10.910	0.393	0.549
ICEdit	0.263	0.388	0.515	0.875	0.845	0.842	0.524	14.537	0.435	0.606
MGIE	0.325	0.580	0.685	0.801	0.710	0.723	0.054	10.508	0.350	0.404
HIVE	0.294	0.484	0.607	0.847	0.771	0.770	0.487	12.415	0.337	0.540
FLUX	0.275	0.478	0.599	0.867	0.860	0.857	0.678	11.903	0.332	0.605
HQEdit	0.317	0.590	0.710	0.819	0.677	0.682	0.524	9.010	0.292	0.501
Step1X	0.250	0.344	0.453	0.896	0.888	0.885	0.610	14.837	0.464	0.654

plication.

$$\text{LPIPS}(x, x_0) = \sum_l \frac{1}{H_l W_l} \sum_{h,w} \|w_l \odot (\hat{F}_{hw}^l(x) - \hat{F}_{hw}^l(x_0))\|_2^2, \quad (1)$$

CLIP Score [21] measures global semantic consistency. It is defined as the cosine similarity between the CLIP image embeddings (E_I).

$$\text{CLIP}(I_1, I_2) = \frac{E_I(I_1) \cdot E_I(I_2)}{\|E_I(I_1)\| \cdot \|E_I(I_2)\|} \quad (2)$$

4.3. Decoupled Regional Fidelity Metrics

Global metrics can average out local errors. We therefore decouple the evaluation into foreground and background regions using the ground-truth mask M_{fg} = M_{gt} and its inverse M_{bg} = $1 - M_{gt}$.

4.3.1. Editing Fidelity

This evaluation compares I_{gen} and I_{gt} within the M_{fg} region. To compute foreground metrics, we first generate masked images I_{gen}^{fg} and I_{gt}^{fg} by zeroing out pixels outside M_{fg} . We then compute **FG-LPIPS** to measure perceptual fidelity and the **FG-CLIP Score** for semantic fidelity.

$$\text{FG-LPIPS} = \text{LPIPS}(I_{gen}^{fg}, I_{gt}^{fg}) \quad (3)$$

$$\text{FG-CLIP} = \text{CLIP}(I_{gen}^{fg}, I_{gt}^{fg}) \quad (4)$$

4.3.2. Background Fidelity

This evaluation quantifies the consistency of the M_{bg} region. Symmetrically, we create I_{gen}^{bg} and I_{gt}^{bg} by setting the foreground pixels to 0. We then compute **BG-LPIPS** and the **BG-CLIP Score** between these two background-only images.

$$\text{BG-LPIPS} = \text{LPIPS}(I_{gen}^{bg}, I_{gt}^{bg}) \quad (5)$$

$$\text{BG-CLIP} = \text{CLIP}(I_{gen}^{bg}, I_{gt}^{bg}) \quad (6)$$

5. Experiment

5.1. Instruction Compliance Metrics

The above metrics measure image-to-image fidelity but cannot assess whether I_{gen} semantically follows the instruction T_{mod} . To address this, we introduce an evaluation that directly links the text instruction with the generated image using automated QA generation and an MLLM referee.

Step 1: Automated QA Pair Generation. For each instruction T_{mod} , we automatically generate 1–3 verifiable QA pairs using gpt-4o, providing a ground-truth answer.

Step 2: MLLM Referee. We input I_{gen} , the question, and ground-truth answer into gpt-4o to perform multimodal verification, asking it to return True or False on

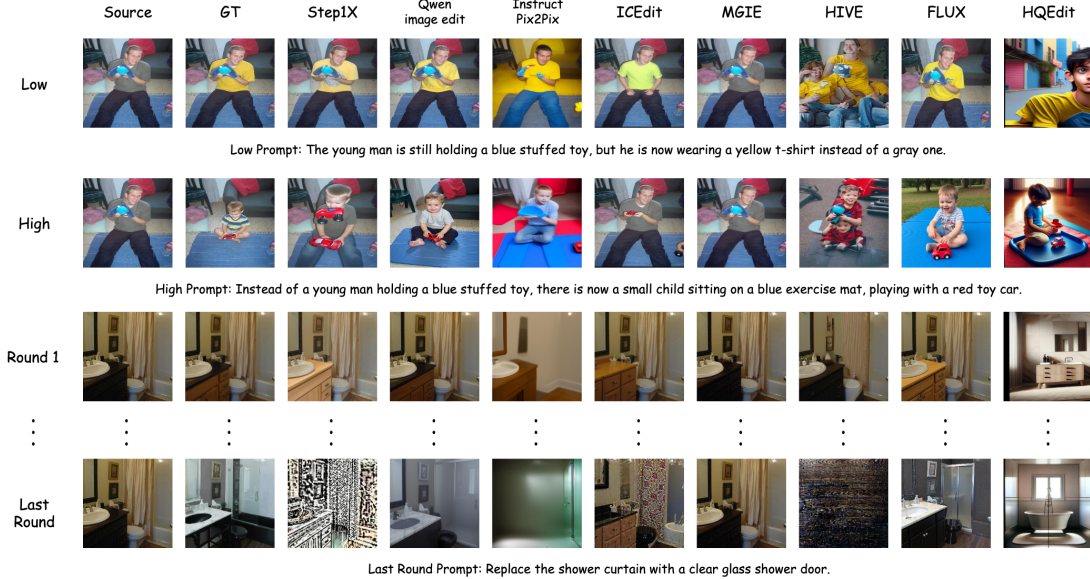


Figure 4. Visualizing Single-Turn and Multi-Turn Consistency Across Multiple Models

whether the answer is semantically correct for the image.

Step 3: Scoring. We use a strict one-strike policy: a sample scores 1.0 only if all its QA pairs are True; if any are False, the score is 0.0, ensuring only fully compliant edits get a high score. In this section, we conduct a comprehensive evaluation of 8 mainstream Instruction-based Image Editing (IIE) models using Omni IIE Bench benchmark.

5.2. Experimental Setup

We selected 8 representative IIE models for evaluation, covering the diverse technical approaches currently available. These include Qwen-image-edit, MGIE, InstructPix2Pix, ICEdit, HIVE, hqedit, FLUX, and Step1X.

Evaluation Metrics. We employ the decoupled evaluation framework defined in Section 4, which includes global image quality metrics, regional fidelity metrics, and instruction compliance metrics.

5.3. Single-turn Consistency Diagnosis

Overall Evaluation Results. As shown in Table 2, Omni IIE Bench reveals significant differences among the models. Qwen-image-edit performs the best, while HQEdit performs the worst. There is a considerable gap between instruction-following ability and image generation quality. For example, although MGIE achieves high image generation quality, its instruction-following capability is very poor. This allows it to score highly on many benchmarks that do not evaluate instruction compliance,

whereas Omni IIE Bench is able to detect this issue. As shown in the examples in Figure 4, Qwen-Image-Edit outperforms the other models, whereas MGIE outputs are almost identical to the original images, demonstrating extremely poor instruction-following ability.

Effect of Semantic Scale Regarding the impact of instruction-editing semantic scales on image editing models, we provide a detailed analysis in Appendix Section B. Please refer to the appendix for full details.

5.4. Multi-turn Coordination Diagnosis

Overall Evaluation Results. Unlike single-turn dialogues, as shown in Table 3, multi-turn generation performance drops for all models due to error accumulation, though Qwen-Image-Edit and Step1X remain relatively strong, while MGIE declines further.

Instruction-following Ability For multi-turn dialogues, to better simulate practical scenarios, the instruction length for each turn is generally shorter, resulting in a significantly lower difficulty for QA generation compared to single-turn dialogues. Consequently, the instruction-following evaluation is inherently easier in this setting. As a result, for the same model, the QA scores in Table 3 are often higher than those in Table 2.

Background Preservation Capability. Comparing Tables 2 and 3, multi-turn dialogues clearly cause a substantial drop in background preservation across all models, primarily due to error accumulation. In real-world

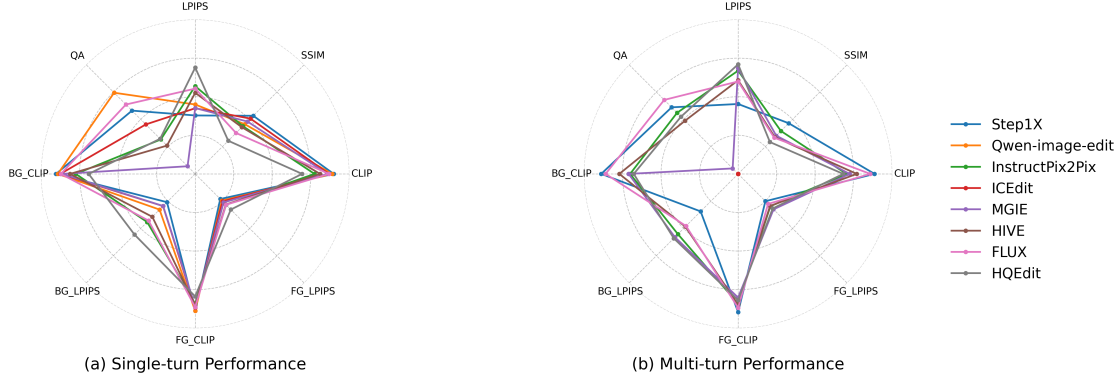


Figure 5. Comparison of 8 IIE models across 8 metrics on Omni IIE Bench. The charts show normalized scores for (a) the Single-turn Consistency task and (b) the Multi-turn Coordination task.

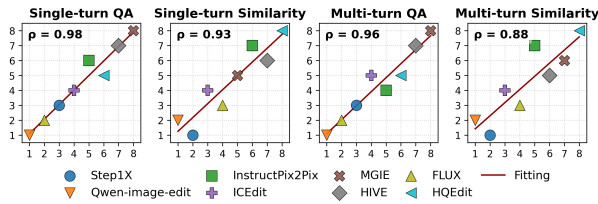


Figure 6. Alignment between Omni IIE Bench ranks (Y-axis) and human evaluation ranks (X-axis).

scenarios, where designers frequently perform multiple edits, such errors accumulate continuously, highlighting a key limitation of current mainstream models, according to Omni IIE Bench.

5.5. Human Alignment

To validate that the evaluation metrics are accurate and representative, we conducted a human alignment assessment experiment. In this experiment, we evaluated the alignment between the metrics and human judgment from two aspects: image similarity and instruction compliance. For instruction compliance, we focused on the ranking according to the model’s QA metric. For image similarity, since humans can only subjectively assess the similarity between two images, we focused on the ranking based on the model’s CLIP metric.

We selected four annotators for this study, including two PhD students in computer science and two professional designers. From the single-turn results generated by each model, we randomly sampled 100 sets, each consisting of the original image, the image generated by *Nano Banana*, and the corresponding instruction. Similarly, from the multi-turn results, we randomly sampled 20 complete multi-turn dialogues, each including the original image, the Nano Banana-generated images, and the corresponding instructions. The four annotators were then asked to score instruction compliance and

similarity to the ground-truth image, using a scale from 1 to 3. The mean score for each sample was calculated, and final rankings were determined based on these mean scores.

We plot the rankings of different models according to Omni IIE Bench against the human rankings in a 2D plot, where the X-axis represents human rankings and the Y-axis represents model rankings. We then compute the correlation coefficient across the corresponding points for each image.

As shown in Figure 6, the rankings of all metrics exhibit a very high correlation with human subjective rankings, with correlation coefficients all above 0.85. This data demonstrates the accuracy and representativeness of Omni IIE Bench evaluation process.

6. Conclusion

This paper addresses a key unresolved issue in current Instruction-based Image Editing (IIE) evaluations: a significant gap exists between benchmark performance and real-world applicability. To tackle this problem, we propose **Omni IIE Bench** — a high-quality, human-annotated diagnostic benchmark designed to assess the practical performance of IIE models.

Omni IIE Bench includes both single turn and multi turn dialogue evaluations, combined with multi-stage human filtering to achieve a comprehensive assessment of model capabilities. We evaluated 8 mainstream IIE models, and the results show that even state-of-the-art models experience significant drops in image fidelity, semantic accuracy, and background preservation when transitioning from low- to high-semantic-scale tasks. Furthermore, in multi-turn dialogues, error accumulation leads to a substantial decline in performance across nearly all models. Omni IIE Bench provides diagnostic tools and insights to guide the development of more practical IIE models.

References

- [1] Samyadeep Basu, Mehrdad Saberi, Shweta Bhardwaj, Atoosa Malemir Chegini, Daniela Massiceti, Maziar Sanjabi, Shell Xu Hu, and Soheil Feizi. Editval: Benchmarking diffusion based text-guided image editing methods. *arXiv preprint arXiv:2310.02426*, 2023. 1, 2, 4
- [2] Stephen Batifol, Andreas Blattmann, Frederic Boesel, Saksham Consul, Cyril Diagne, Tim Dockhorn, Jack English, Zion English, Patrick Esser, Sumith Kulal, et al. Flux. 1 kontekst: Flow matching for in-context image generation and editing in latent space. *arXiv e-prints*, pages arXiv–2506, 2025. 1, 6
- [3] Tim Brooks, Aleksander Holynski, and Alexei A Efros. Instructpix2pix: Learning to follow image editing instructions. In *Proceedings of the IEEE/CVF conference on computer vision and pattern recognition*, pages 18392–18402, 2023. 1, 6
- [4] Guiming Hardy Chen, Shunian Chen, Ruifei Zhang, Junying Chen, Xiangbo Wu, Zhiyi Zhang, Zhihong Chen, Jianquan Li, Xiang Wan, and Benyou Wang. Allava: Harnessing gpt4v-synthesized data for lite vision-language models. *arXiv preprint arXiv:2402.11684*, 2024. 3
- [5] Junying Chen, Zhenyang Cai, Pengcheng Chen, Shunian Chen, Ke Ji, Xidong Wang, Yunjin Yang, and Benyou Wang. Sharegpt-4o-image: Aligning multimodal models with gpt-4o-level image generation. *arXiv preprint arXiv:2506.18095*, 2025. 3
- [6] Lin Chen, Jinsong Li, Xiaoyi Dong, Pan Zhang, Conghui He, Jiaqi Wang, Feng Zhao, and Dahua Lin. Sharegpt4v: Improving large multi-modal models with better captions. In *European Conference on Computer Vision*, pages 370–387. Springer, 2024. 3
- [7] Tsu-Jui Fu, Wenze Hu, Xianzhi Du, William Yang Wang, Yinfei Yang, and Zhe Gan. Guiding Instruction-based Image Editing via Multimodal Large Language Models. In *International Conference on Learning Representations (ICLR)*, 2024. 1, 6
- [8] Roopal Garg, Andrea Burns, Burcu Karagol-Ayan, Yonatan Bitton, Ceslee Montgomery, Yasumasa Onoe, Andrew Bunner, Ranjay Krishna, Jason Michael Baldrige, and Radu Soricut. Imageinwords: Unlocking hyper-detailed image descriptions. In *Proceedings of the 2024 Conference on Empirical Methods in Natural Language Processing*, pages 93–127, 2024. 3
- [9] Drew A Hudson and Christopher D Manning. Gqa: A new dataset for real-world visual reasoning and compositional question answering. In *Proceedings of the IEEE/CVF conference on computer vision and pattern recognition*, pages 6700–6709, 2019. 3
- [10] Mude Hui, Siwei Yang, Bingchen Zhao, Yichun Shi, Heng Wang, Peng Wang, Yuyin Zhou, and Cihang Xie. Hq-edit: A high-quality dataset for instruction-based image editing. *arXiv preprint arXiv:2404.09990*, 2024. 1, 6
- [11] Bohan Jia, Wenxuan Huang, Yuntian Tang, Junbo Qiao, Jincheng Liao, Shaosheng Cao, Fei Zhao, Zhaopeng Feng, Zhouhong Gu, Zhenfei Yin, et al. Compbench: Benchmarking complex instruction-guided image editing. *arXiv preprint arXiv:2505.12200*, 2025. 1, 2, 4
- [12] Alexander Kirillov, Eric Mintun, Nikhila Ravi, Hanzi Mao, Chloe Rolland, Laura Gustafson, Tete Xiao, Spencer Whitehead, Alexander C. Berg, Wan-Yen Lo, Piotr Dollár, and Ross Girshick. Segment anything. *arXiv:2304.02643*, 2023. 3
- [13] Tsung-Yi Lin, Michael Maire, Serge Belongie, James Hays, Pietro Perona, Deva Ramanan, Piotr Dollár, and C Lawrence Zitnick. Microsoft coco: Common objects in context. In *European conference on computer vision*, pages 740–755. Springer, 2014. 3
- [14] Haotian Liu, Chunyuan Li, Qingyang Wu, and Yong Jae Lee. Visual instruction tuning. *Advances in neural information processing systems*, 36:34892–34916, 2023. 3
- [15] Shilong Liu, Zhaoyang Zeng, Tianhe Ren, Feng Li, Hao Zhang, Jie Yang, Chunyuan Li, Jianwei Yang, Hang Su, Jun Zhu, et al. Grounding dino: Marrying dino with grounded pre-training for open-set object detection. *arXiv preprint arXiv:2303.05499*, 2023. 3
- [16] Shiyu Liu, Yucheng Han, Peng Xing, Fukun Yin, Rui Wang, Wei Cheng, Jiaqi Liao, Yingming Wang, Honghao Fu, Chunrui Han, Guopeng Li, Yuang Peng, Quan Sun, Jingwei Wu, Yan Cai, Zheng Ge, Ranchen Ming, Lei Xia, Xianfang Zeng, Yibo Zhu, Binxing Jiao, Xiangyu Zhang, Gang Yu, and Daxin Jiang. Step1x-edit: A practical framework for general image editing. *arXiv preprint arXiv:2504.17761*, 2025. 1, 6
- [17] Google LLC. Gemini 2.5 flash image (a.k.a. “nano banana”)–image generation & editing model. <https://cloud.google.com/blog/products/ai-machine-learning/gemini-2-5-flash-image/>, 2025. Accessed: 2025-11-12. 3
- [18] Yiwei Ma, Jiayi Ji, Ke Ye, Weihuang Lin, Zhibin Wang, Yonghan Zheng, Qiang Zhou, Xiaoshuai Sun, and Rongrong Ji. I2ebench: A comprehensive benchmark for instruction-based image editing. *Advances in Neural Information Processing Systems*, 37:41494–41516, 2024. 1, 2, 4
- [19] Yasumasa Onoe, Sunayana Rane, Zachary Berger, Yonatan Bitton, Jaemin Cho, Roopal Garg, Alexander Ku, Zarana Parekh, Jordi Pont-Tuset, Garrett Tanzer, et al. Docci: Descriptions of connected and contrasting images. In *European Conference on Computer Vision*, pages 291–309. Springer, 2024. 3
- [20] OpenAI, :, Aaron Hurst, Adam Lerer, Adam P. Goucher, Adam Perelman, Aditya Ramesh, Aidan Clark, AJ Ostrow, Akila Welihinda, Alan Hayes, Alec Radford, Aleksander Mądry, Alex Baker-Whitcomb, Alex Beutel, Alex Borzunov, Alex Carney, Alex Chow, Alex Kirillov, Alex Nichol, Alex Paino, Alex Renzin, Alex Tachard Passos, Alexander Kirillov, Alexi Christakis, Alexis Conneau, Ali Kamali, Allan Jabri, Allison Moyer, Allison Tam, Amadou Crookes, Amin Tootoochian, Amin Tootoonchian, Ananya Kumar, Andrea Vallone, Andrej Karpathy, Andrew Braunstein, Andrew Cann, Andrew Codisoti, Andrew Galu, Andrew Kondrich, Andrew Tulloch, Andrey Mishchenko, Angela Baek, Angela Jiang, Antoine Pelisse, Antonia Woodford, Anuj

- Gosalia, Arka Dhar, Ashley Pantuliano, Avi Nayak, Avital Oliver, Barret Zoph, Behrooz Ghorbani, Ben Leimberger, Ben Rossen, Ben Sokolowsky, Ben Wang, Benjamin Zweig, Beth Hoover, Blake Samic, Bob McGrew, Bobby Spero, Bogo Gierler, Bowen Cheng, Brad Lightcap, Brandon Walkin, Brendan Quinn, Brian Guarraci, Brian Hsu, Bright Kellogg, Brydon Eastman, Camillo Lugaresi, and Carroll Wainwright at al. Gpt-4o system card, 2024. 3
- [21] Alec Radford, Jong Wook Kim, Chris Hallacy, Aditya Ramesh, Gabriel Goh, Sandhini Agarwal, Girish Sastry, Amanda Askell, Pamela Mishkin, Jack Clark, et al. Learning transferable visual models from natural language supervision. In *International conference on machine learning*, pages 8748–8763. PmLR, 2021. 6
- [22] Tianhe Ren, Shilong Liu, Ailing Zeng, Jing Lin, Kunchang Li, He Cao, Jiayu Chen, Xinyu Huang, Yukang Chen, Feng Yan, Zhaoyang Zeng, Hao Zhang, Feng Li, Jie Yang, Hongyang Li, Qing Jiang, and Lei Zhang. Grounded sam: Assembling open-world models for diverse visual tasks, 2024. 3
- [23] Babak Saleh and Ahmed Elgammal. Large-scale classification of fine-art paintings: Learning the right metric on the right feature. *arXiv preprint arXiv:1505.00855*, 2015. 3
- [24] Shelly Sheynin, Adam Polyak, Uriel Singer, Yuval Kirstain, Amit Zohar, Oron Ashual, Devi Parikh, and Yaniv Taigman. Emu edit: Precise image editing via recognition and generation tasks. In *Proceedings of the IEEE/CVF Conference on Computer Vision and Pattern Recognition*, pages 8871–8879, 2024. 1, 2, 4
- [25] Vasu Singla, Kaiyu Yue, Sukriti Paul, Reza Shirkanvand, Mayuka Jayawardhana, Alireza Ganjdanesh, Heng Huang, Abhinav Bhatel, Gowthami Somepalli, and Tom Goldstein. From pixels to prose: A large dataset of dense image captions. *arXiv preprint arXiv:2406.10328*, 2024. 3
- [26] Pei Wang, Yanan Wu, Zekun Wang, Jiaheng Liu, Xiaoshuai Song, Zhongyuan Peng, Ken Deng, Chenchen Zhang, Jiakai Wang, Junran Peng, Ge Zhang, Hangyu Guo, Zhaoxiang Zhang, Wenbo Su, and Bo Zheng. Mtu-bench: A multi-granularity tool-use benchmark for large language models, 2024. 1
- [27] Su Wang, Chitwan Saharia, Ceslee Montgomery, Jordi Pont-Tuset, Shai Noy, Stefano Pellegrini, Yasumasa Onoe, Sarah Laszlo, David J Fleet, Radu Soricut, et al. Imagen editor and editbench: Advancing and evaluating text-guided image inpainting. In *Proceedings of the IEEE/CVF conference on computer vision and pattern recognition*, pages 18359–18369, 2023. 1, 2, 4
- [28] Xinming Wang, Jian Xu, Aslan H Feng, Yi Chen, Haiyang Guo, Fei Zhu, Yuanqi Shao, Minsi Ren, Hongzhu Yi, Sheng Lian, et al. The hitchhiker’s guide to autonomous research: A survey of scientific agents. *Authorea Preprints*, 2025. 2
- [29] Xinming Wang, Jian Xu, Bin Yu, Sheng Lian, Hongzhu Yi, Yi Chen, Yingjian Zhu, Boran Wang, Hongming Yang, Han Hu, et al. Mr-align: Meta-reasoning informed factuality alignment for large reasoning models. *arXiv preprint arXiv:2510.24794*, 2025. 2
- [30] Zhou Wang, Alan C Bovik, Hamid R Sheikh, and Eero P Simoncelli. Image quality assessment: from error visibility to structural similarity. *IEEE transactions on image processing*, 13(4):600–612, 2004. 5
- [31] Zhepeng Wang, Yingjian Zhu, Guanghao Dong, Hongzhu Yi, Feng Chen, Xinming Wang, and Jun Xie. Multimodal video emotion recognition with reliable reasoning priors. *arXiv preprint arXiv:2508.03722*, 2025. 1
- [32] Chenfei Wu, Jiahao Li, Jingren Zhou, Junyang Lin, Kaiyuan Gao, Kun Yan, Sheng ming Yin, Shuai Bai, Xiao Xu, Yilei Chen, Yuxiang Chen, Zecheng Tang, Zekai Zhang, Zhengyi Wang, An Yang, Bowen Yu, Chen Cheng, Dayiheng Liu, Deqing Li, Hang Zhang, Hao Meng, Hu Wei, Jingyuan Ni, Kai Chen, Kuan Cao, Liang Peng, Lin Qu, Minggang Wu, Peng Wang, Shuting Yu, Tingkun Wen, Wensen Feng, Xiaoxiao Xu, Yi Wang, Yichang Zhang, Yongqiang Zhu, Yujia Wu, Yuxuan Cai, and Zenan Liu. Qwen-image technical report, 2025. 1, 6
- [33] Shirley Wu, Michel Galley, Baolin Peng, Hao Cheng, Gavin Li, Yao Dou, Weixin Cai, James Zou, Jure Leskovec, and Jianfeng Gao. Collabllm: From passive responders to active collaborators, 2025. 1
- [34] Jianxiong Xiao, James Hays, Krista A Ehinger, Aude Oliva, and Antonio Torralba. Sun database: Large-scale scene recognition from abbey to zoo. In *2010 IEEE computer society conference on computer vision and pattern recognition*, pages 3485–3492. IEEE, 2010. 3
- [35] Jun Xie, Xiaohui Fan, Zhenghao Zhang, Feng Chen, Hongzhu Yi, Yingjian Zhu, Xiongjun Guan, Xinming Wang, Yue Bi, Tao Zhang, et al. Zeroes: Zero-shot ensemble for open-vocabulary video emotion recognition with large multimodal models. In *Proceedings of the 3rd International Workshop on Multimodal and Responsible Affective Computing*, pages 23–29, 2025. 2
- [36] Jun Xie, Yingjian Zhu, Feng Chen, Zhenghao Zhang, Xiaohui Fan, Hongzhu Yi, Xinming Wang, Chen Yu, Yue Bi, Zhaoran Zhao, et al. More is better: A moe-based emotion recognition framework with human preference alignment. In *Proceedings of the 3rd International Workshop on Multimodal and Responsible Affective Computing*, pages 2–7, 2025. 1
- [37] Yang Ye, Xianyi He, Zongjian Li, Bin Lin, Shenghai Yuan, Zhiyuan Yan, Bohan Hou, and Li Yuan. Imgedit: A unified image editing dataset and benchmark. *arXiv preprint arXiv:2505.20275*, 2025. 1, 2, 4
- [38] Hongzhu Yi, Xinming Wang, Tianyu Zong, Yuanxiang Wang, Jun Xie, Tao Yu, Haopeng Jin, Zhepeng Wang, Kaixin Xu, Feng Chen, et al. Rpo: Reinforcement fine-tuning with partial reasoning optimization. *arXiv preprint arXiv:2601.19404*, 2026. 1
- [39] Peter Young, Alice Lai, Micah Hodosh, and Julia Hockenmaier. From image descriptions to visual denotations: New similarity metrics for semantic inference over event descriptions. *Transactions of the association for computational linguistics*, 2:67–78, 2014. 3

- [40] Qifan Yu, Wei Chow, Zhongqi Yue, Kaihang Pan, Yang Wu, Xiaoyang Wan, Juncheng Li, Siliang Tang, Hanwang Zhang, and Yueting Zhuang. Anyedit: Mastering unified high-quality image editing for any idea. In *Proceedings of the IEEE/CVF Conference on Computer Vision and Pattern Recognition (CVPR)*, pages 26125–26135, 2025. 1, 4
- [41] Tao Yu, Zhengbo Zhang, Zhiheng Lyu, Junhao Gong, Hongzhu Yi, Xinming Wang, Yuxuan Zhou, Jiabing Yang, Ping Nie, Yan Huang, and Wenhui Chen. Browser-agent — learning human-inspired web browsing for effective information search, 2025. 1
- [42] Tao Yu, Haopeng Jin, Hao Wang, Shenghua Chai, Yujia Yang, Junhao Gong, Jiaming Guo, Minghui Zhang, Xinlong Chen, Zhenghao Zhang, et al. Shotfinder: Imagination-driven open-domain video shot retrieval via web search. *arXiv preprint arXiv:2601.23232*, 2026. 1
- [43] Kai Zhang, Lingbo Mo, Wenhui Chen, Huan Sun, and Yu Su. Magicbrush: A manually annotated dataset for instruction-guided image editing. *Advances in Neural Information Processing Systems*, 36:31428–31449, 2023. 1, 2, 4
- [44] Richard Zhang, Phillip Isola, Alexei A Efros, Eli Shechtman, and Oliver Wang. The unreasonable effectiveness of deep features as a perceptual metric. In *Proceedings of the IEEE conference on computer vision and pattern recognition*, pages 586–595, 2018. 5
- [45] Shu Zhang, Xinyi Yang, Yihao Feng, Can Qin, Chia-Chih Chen, Ning Yu, Zeyuan Chen, Huan Wang, Silvio Savarese, Stefano Ermon, et al. Hive: Harnessing human feedback for instructional visual editing. In *Proceedings of the IEEE/CVF Conference on Computer Vision and Pattern Recognition*, pages 9026–9036, 2024. 1, 6
- [46] Zhenghao Zhang, Jun Xie, Xingchen Chen, Tao Yu, Hongzhu Yi, Kaixin Xu, Yuanxiang Wang, Tianyu Zong, Xinming Wang, Jiahuan Chen, et al. Dynamic deep graph learning for incomplete multi-view clustering with masked graph reconstruction loss. *arXiv preprint arXiv:2511.11181*, 2025. 2
- [47] Zechuan Zhang, Ji Xie, Yu Lu, Zongxin Yang, and Yi Yang. In-context edit: Enabling instructional image editing with in-context generation in large scale diffusion transformer. *arXiv preprint arXiv:2504.20690*, 2025. 1, 6
- [48] Zijun Zhou, Yingying Deng, Xiangyu He, Weiming Dong, and Fan Tang. Multi-turn consistent image editing. *arXiv preprint arXiv:2505.04320*, 2025. 1, 2, 4
- [49] Tianyu Zong, Bingkang Shi, Hongzhu Yi, and Jungang Xu. Tncse: Tensor norm constraints for unsupervised contrastive learning of sentence embeddings. In *Proceedings of the AAAI Conference on Artificial Intelligence*, pages 26192–26201, 2025.
- [50] Tianyu Zong, Hongzhu Yi, Bingkang Shi, Yuanxiang Wang, and Jungang Xu. Jtcse: Joint tensor-modulus constraints and cross-attention for unsupervised contrastive learning of sentence embeddings. *arXiv preprint arXiv:2505.02366*, 2025. 2

Appendix

A. Cases of Omni IIE Bench

This section presents several GT images and their corresponding instructions for single-turn dialogues, including examples of edits at both low and high semantic scales as shown in Figures 7 and 8.

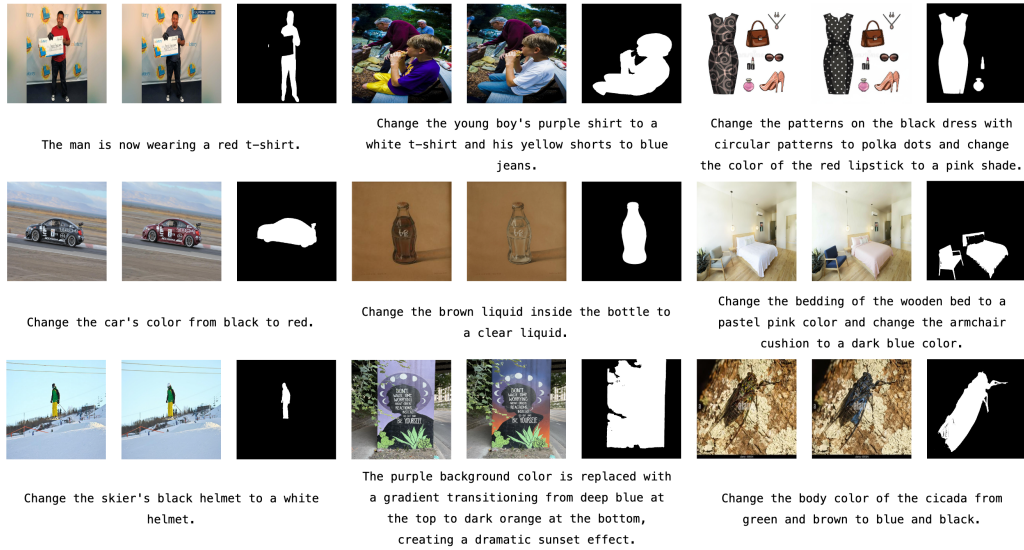


Figure 7. Cases of Single Turn Low

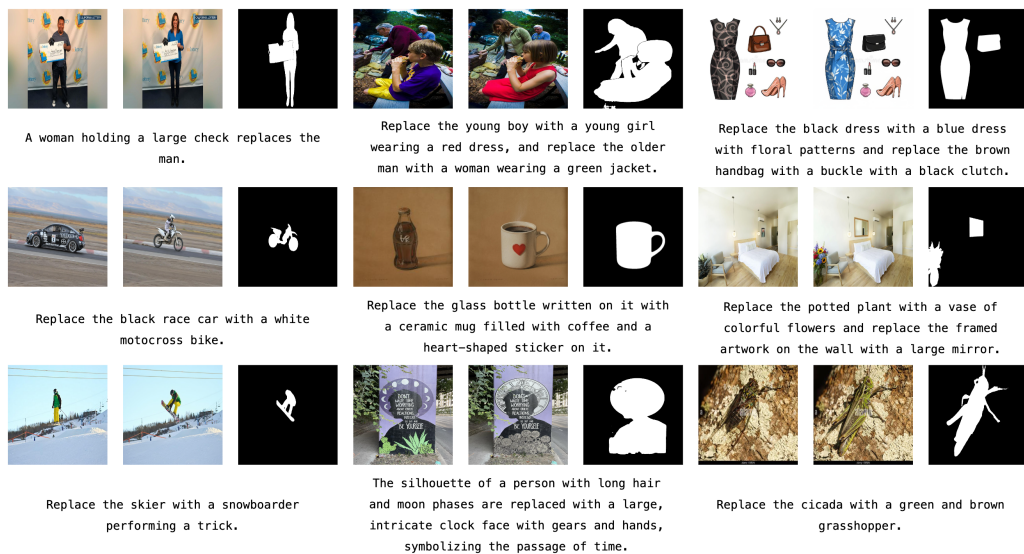


Figure 8. Cases of Single Turn High

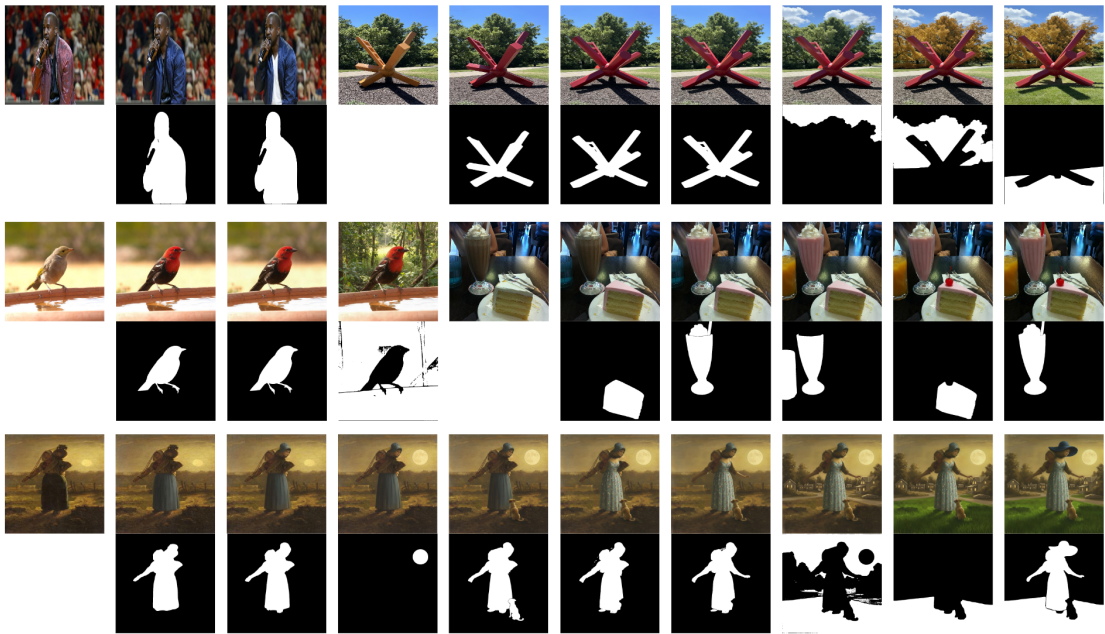


Figure 9. Cases of Multi Turn

B. Single-Turn Dialogue Metric Details

This section presents the metric details of different models at low and high semantic scales during single-turn dialogues. Overall, regardless of the model, edits at a high semantic scale perform worse than those at a low semantic scale. The specific details are shown in Tables 4 and 5.

Table 4. Performance comparison of IIE models on the Low group (metrics grouped by category). Text colors indicate top performances: 1st, 2nd, 3rd. Arrows (\uparrow / \downarrow) indicate whether higher or lower values are better. The Overall score is calculated by the formula $\frac{1}{4} \left[\frac{3 - (\sum \text{LPIPS})}{3} + \frac{\sum \text{CLIP}}{3} + \text{QA} + \text{SSIM} \right]$, where $\sum \text{LPIPS}$ and $\sum \text{CLIP}$ are the sums of their respective FG, BG, and ALL columns.

Model	LPIPS (\downarrow)			CLIP (\uparrow)			QA (\uparrow)	Image Quality (\uparrow)		Overall
	FG	BG	ALL	FG	BG	ALL		PSNR	SSIM	
Qwen-image-edit	0.231	0.299	0.414	0.910	0.899	0.910	0.780	15.323	0.474	0.710
Instruct_Pix2Pix	0.284	0.435	0.555	0.861	0.797	0.796	0.400	12.476	0.443	0.559
ICEdit	0.250	0.311	0.407	0.888	0.896	0.889	0.550	16.107	0.519	0.662
MGIE	0.264	0.294	0.406	0.894	0.898	0.895	0.080	15.328	0.495	0.539
HIVE	0.283	0.376	0.505	0.873	0.836	0.836	0.300	14.257	0.444	0.551
FLUX	0.287	0.422	0.545	0.878	0.891	0.888	0.720	12.769	0.376	0.641
HQEdit	0.314	0.539	0.671	0.810	0.711	0.713	0.420	9.504	0.314	0.491
Step1X	0.218	0.244	0.353	0.912	0.923	0.920	0.650	16.663	0.547	0.711

Table 5. Performance comparison of IIE models on the High group (metrics grouped by category). Text colors indicate top performances: 1st, 2nd, 3rd. Arrows (\uparrow / \downarrow) indicate whether higher or lower values are better. Arrows (\uparrow / \downarrow) indicate whether higher or lower values are better. The Overall score is calculated by the formula $\frac{1}{4} \left[\frac{3 - (\sum \text{LPIPS})}{3} + \frac{\sum \text{CLIP}}{3} + \text{QA} + \text{SSIM} \right]$, where $\sum \text{LPIPS}$ and $\sum \text{CLIP}$ are the sums of their respective FG, BG, and ALL columns.

Model	LPIPS (\downarrow)			CLIP (\uparrow)			QA (\uparrow)	Image Quality (\uparrow)		Overall
	FG	BG	ALL	FG	BG	ALL		PSNR	SSIM	
Qwen-image-edit	0.264	0.360	0.495	0.859	0.866	0.866	0.710	13.241	0.431	0.657
Instruct_Pix2Pix	0.283	0.448	0.586	0.816	0.749	0.747	0.230	12.356	0.431	0.498
ICEdit	0.254	0.311	0.448	0.840	0.849	0.842	0.360	14.830	0.492	0.589
MGIE	0.264	0.313	0.452	0.813	0.821	0.813	0.060	13.983	0.461	0.499
HIVE	0.278	0.415	0.552	0.819	0.783	0.778	0.220	13.122	0.407	0.501
FLUX	0.277	0.436	0.562	0.844	0.848	0.844	0.550	12.282	0.373	0.586
HQEdit	0.316	0.578	0.711	0.774	0.668	0.670	0.220	8.952	0.291	0.420
Step1X	0.247	0.278	0.411	0.857	0.878	0.872	0.510	14.818	0.515	0.646

C. Examples of Image Descriptions and Editing Instructions

This section presents several image descriptions and editing instructions generated during the construction of Omni IIE Bench.

```
{
  "replaceable_subject": {
    "name": "a hooded figure in a brown robe"
  },
  "modifiable_attributes": {
    "subject": [
      "robe is brown",
      "figure is hooded",
      "hands are clasped",
      "posture is upright"
    ],
    "background": [
      "background is dark and shadowy",
      "lighting is dramatic and focused on the figure"
    ]
  }
}
```

Listing 1. Example description JSON in our benchmark.

```
{
  "replaceable_subject": {
    "name": "a brown bird with a long tail"
  },
  "modifiable_attributes": {
    "subject": [
      "feathers are brown",
      "tail is long and dark",
      "beak is curved and pointed",
      "legs are slender and gray"
    ],
    "background": [
      "floor is tiled and beige",
      "pillar is gray and cylindrical",
      "partial view of a black object (possibly a chair or table)"
    ]
  }
}
```

Listing 2. Example description JSON in our benchmark.

```

{
  "replaceable_subject": {
    "name": "a modern bathroom interior"
  },
  "modifiable_attributes": {
    "subject": [
      "vanity cabinet is dark wood",
      "sink is white ceramic",
      "toilet is white ceramic",
      "shower curtain is beige with a floral pattern",
      "tub is white ceramic",
      "mirror is framed in gold"
    ],
    "background": [
      "walls are painted beige",
      "floor is light wood",
      "lighting is warm and ambient"
    ]
  }
}

```

Listing 3. Example description JSON in our benchmark.

```

{
  "modifications": [
    {
      "level": "low",
      "modification_text": "Change the color of the robe from brown to black."
    },
    {
      "level": "high",
      "modification_text": "Replace the hooded figure in a brown robe with a
↔ cloaked wizard wearing a pointy hat."
    }
  ]
}

```

Listing 4. Example single-turn modification JSON in our benchmark.

```

{
  "modifications": [
    {
      "level": "low",
      "modification_text": "Change the feathers of the brown bird to be white."
    },
    {
      "level": "high",
      "modification_text": "Replace the brown bird with a gray rabbit."
    }
  ]
}

```

Listing 5. Example single-turn modification JSON in our benchmark.

```

{
  "modifications": [
    {
      "level": "1",
      "modification_text": "Change the color of the vanity cabinet to a lighter
↪ oak tone."
    },
    {
      "level": "2",
      "modification_text": "Replace the floral pattern of the shower curtain
↪ with a geometric pattern."
    },
    {
      "level": "3",
      "modification_text": "Change the lighting to a cooler, brighter tone."
    },
    {
      "level": "4",
      "modification_text": "Replace the gold frame of the mirror with a silver
↪ frame."
    },
    {
      "level": "5",
      "modification_text": "Change the color of the walls to a light gray."
    },
    {
      "level": "6",
      "modification_text": "Replace the white ceramic sink with a black granite
↪ sink."
    },
    {
      "level": "7",
      "modification_text": "Change the floor to a darker wood tone."
    },
    {
      "level": "8",
      "modification_text": "Replace the white ceramic toilet with a black
↪ ceramic toilet."
    },
    {
      "level": "9",
      "modification_text": "Change the white ceramic tub to a black granite
↪ tub."
    },
    {
      "level": "10",
      "modification_text": "Replace the light gray walls with a dark gray
↪ color."
    },
    {
      "level": "11",
      "modification_text": "Replace the vanity cabinet with a marble countertop
↪ and a black frame."
    },
    {
      "level": "12",
      "modification_text": "Replace the shower curtain with a clear glass shower
↪ door."
    }
  ]
}

```

Listing 6. Example multi-turn modification JSON in our benchmark.